

Whole Body Low Dose Computed Tomography Using Third-Generation Dual-Source Multidetector With Spectral Shaping: Protocol Optimization and Literature Review

Dario Baldi¹ , Liberatore Tramontano¹, Vincenzo Alfano¹, Bruna Punzo¹, Carlo Cavaliere¹, and Marco Salvatore¹

Abstract

For decades, the main imaging tool for multiple myeloma (MM) patient's management has been the conventional skeleton survey. In 2014 international myeloma working group defined the advantages of the whole-body low dose computed tomography (WBLDCT) as a gold standard, among imaging modalities, for bone disease assessment and subsequently implemented this technique in the MM diagnostic workflow. The aim of this study is to investigate, in a group of 30 patients with a new diagnosis of MM, the radiation dose (CT dose index, dose-length product, effective dose), the subjective image quality score and osseous/extra-osseous findings rate with a modified WBLDCT protocol. Spectral shaping and third-generation dual-source multidetector CT scanner was used for the assessment of osteolytic lesions due to MM, and the dose exposure was compared with the literature findings reported until 2020. Mean radiation dose parameters were reported as follows: CT dose index 0.3 ± 0.1 mGy, Dose-Length Product 52.0 ± 22.5 mGy*cm, effective dose 0.44 ± 0.19 mSv. Subjective image quality was good/excellent in all subjects. 11/30 patients showed osteolytic lesions, with a percentage of extra-osseous findings detected in 9/30 patients. Our data confirmed the advantages of WBLDCT in the diagnosis of patients with MM, reporting an effective dose for our protocol as the lowest among previous literature findings.

Keywords

whole-body CT, spectral shaping, radiation dose, image quality, multiple myeloma

Introduction

Bone involvement is one of the signs of multiple myeloma (MM), characterized by an increased activity of osteoclasts and a suppression of osteoblast function, determining bone resorption.¹ Up to 80% of newly diagnosed MM patients have osteolytic lesions, improving the risk of related skeletal events.²

For decades, the primary imaging tool in patients with MM was a conventional skeletal survey (CSS), with significantly lower sensitivity than cross-sectional imaging techniques for diagnosing osteolytic lesions.^{3,4} Furthermore, previous publications ascertained that the sensitivity of conventional X-rays for the evaluation of bone damage was limited since the changes can be detected only with at least 30-50% of the bone mass were destroyed.⁵ CSS is also inadequate for the representation of small lytic lesions,⁶ with a false-negative rate of

30-70%. Furthermore, the positions required for simple radiographs are uncomfortable.⁷

For this reason, computed tomography (CT) was included in the updated MM criteria. According to the new International Myeloma Working Group criteria for MM, numerous studies show that CT has a higher sensitivity than CSS for the detection of multiple bone lesions to myeloma.⁸ Most of these studies

¹ IRCCS SDN, Naples, Italy

Received 07 August 2020; received revised 28 September 2020; accepted 12 October 2020

Corresponding Author:

Dario Baldi, IRCCS SDN, via E.Gianturco 113, 80143, Naples, Italy.
Email: dario.baldi@synlab.it



focused on the whole-body low dose computed tomography (WBLDCT) protocols, which offers the advantage of both full-body coverage and the lower radiation dose delivered to the patient.⁷⁻⁹ For these reasons, recent efforts have been spent to set-up and improve WBLDCT protocol, taking into account technological challenges represented by scanner evolution and parameters optimization (kV, mAs). In this study, we optimize and propose a WBLDCT imaging protocol in patients with suspected plasma cell dyscrasia, reducing radiation dose exposure, but preserving image quality and both skeletal and extra-osseous findings detection.

Materials and Methods

From October 2019 to July 2020 a total of 30 consecutive patients (16 male, 14 female, aged between 43 and 81, mean age 64.3) with clinically confirmed MM underwent unenhanced WBLDCT on a third-generation Dual Source Computed Tomography Somatom Force (Siemens Healthineers, Erlangen, Germany). Informed consent was obtained from the patients, and the local ethics committee (Comitato etico IRCCS Pascale—Naples) approved the study (project identification code: 9_19).

All patients were positioned supine with the arms placed along the trunk in order to include the elbows in the field of view (FOV). Whole-body scanning FOV was adapted to the length and circumference of the patients. All patients were scanned in craniocaudal sense from skull to feet, and acquired in a single inspiratory breath-hold throughout the scan, with a mean acquisition time of about 20 seconds. CT scan parameters were: gantry rotation time, 0.5 s; collimation, 192×0.6 mm, using a z-flying focal spot and automated tube current modulation (Siemens, Care Dose 4D); voltage, 100 kV with additional hardening of the spectrum from a tin filter mounted; reference tube current-time product of 80 mAs; single tube acquisition; pitch of approximately 1.5.

For image reconstruction, an Advanced Modeled Iterative Reconstruction (ADMIRE, Siemens Healthineers) was used with a strength of 3 (available strength of ADMIRE: 1 to 5, where a higher number implies a stronger noise reduction). Then, raw data images were reconstructed in 1.5 mm slice thickness using a Br64 kernel to generate axial images, while 1 mm slice thickness to generate coronal images of the whole body and sagittal images of the spine through multiplanar reformation (MPR). The dose report, with CT dose index (CTDI) and Dose-Length Product (DLP) for the WBLDCT protocol, as defined above, were read from the examination summary reports produced by the CT scanner for each patient, while the dose effects were calculated by multiplying DLP for a whole-body absorption rate constant (0.00842),¹⁰ for each patient. Moreover, a literature analysis was performed in order to compare the dose report obtained with the literature standard until 2020 (Table 1).

Image Quality Assessment

For analysis, image datasets were transferred to an off-line workstation (Syngo.via Workstation; Siemens Healthcare).

Subjective image quality was independently evaluated on a per-region basis by 2 independent radiologists with experience in CT imaging of more than 5 years. During the CT image interpretation session, the overall quality of axial slices, and MPR were assessed. A 4-point scale was used (1 excellent = absence of artifacts; 2 good = minimal artifacts, mild blurring or structure discontinuity but fully evaluable; 3 suboptimal = moderate artifacts and blurring or structure discontinuity; 4 not diagnostic = doubling or discontinuity in the course of the segment preventing diagnostic evaluation.²⁵ In case of disagreement between the observers, consensus was reached in a joint reading to determine the final image quality score. A per-patient image quality score was defined as the worst score found in any region for each patient.

Search Strategy and Selection Criteria

A systematic search for all published studies concerning the application of WBLDCT was conducted. The most relevant scientific electronic databases (PubMed, Cochrane Library, MEDLINE, ScienceDirect, Google Scholar) were comprehensively explored and used to build the search. Only studies published since 2000 were selected, using key terms as “WBLDCT,” “WBCT” and “whole-body-CT.”

Literature search was restricted to English language publications. Two reviewers, after having independently screened identified titles and abstracts, assessed the full text of the original articles involving WBLDCT applications. For articles meeting these criteria with full text available, the following further selection criteria were used: articles were excluded if they involved also preclinical datasets or phantoms and if they were off topic after investigating the full text. The entire flow and results of the literature research were finally checked by a third researcher, in accordance with the Preferred Reporting Items for Systematic Reviews and Meta-Analyses (PRISMA) statement.

Results

The analysis on radiation exposure of the patients showed a mean DLP of 52.0 ± 22.5 mGy*cm, mean CTDI 0.3 ± 0.1 mGy, and a mean dose effective 0.44 ± 0.19 mSv. Subjective image quality, regardless of the disease stage during the examination, was good/excellent in all subjects (median: 1).

The frequency of osteolytic lesion were detected as follows: 11 patients showed presence of osteolytic lesions, among which 5 also with extra-osseous findings (colic diverticulosis, abdominal aortic ectasia, bronchiectasis, pulmonary nodulations, splenomegaly); 19 patients showed no osteolytic lesions, including 4/19 patients with extra-osseous findings (epiaortic or abdominal aortic ectasia, ectopic kidney, hepatomegaly, cholelithiasia) (Figure 1).

Discussion

The survival rate of MM patients has improved in the last few years because of the availability of innovative therapy

Table 1. WBLDCT protocols and studies

Articles	Middle age	Number of patients	Manufacturer	Kv	mAs	Reconstruction Filter	Pitch	Slice thickness	Length of scan	Dlp (mGy*cm)	Dose WBLDCT (mSv)	Dose CSS (mSv)
Horger et al. 2005 ⁶	63.5	100	Somatom Sensation 16 slice Siemens	120	40/50/60/70	B40.B50.B60	/	2 mm	1530.6 mm	/	4.1	/
Chassang et al. 2007 ¹¹	73.4	111	Lightspeed 8 and 64 slices GE (General Electric)	/	/	/	/	/	cervical segment to pelvic bones	609.84 (64 slices) 532.87 (8 slices)	/	/
Kröpil et al. 2008 ⁴	57	29	SOMATOM sensation Cardiac 64 (Siemens)	100	100	B70f	1.4 mm	2 mm	skull to knee joints	408.5 ± 57.55	4.8	/
Gleeson et al. 2008 ⁷	/	39	16-slice MDCT (Siemens Biograph PETCT)	140	14	B60 f (bone)	1.88 mm	3 mm	170 cm length	/	3.3	1.7
Princewill et al. 2013 ¹²	/	51	16 slice Philips Gemini PET/TC	120	100	B kernel	0.813 mm	3 mm	skull—pelvis	/	4.1	1.8
Ippolito et al. 2013 ¹³	63.5	138	16-slice CT (Brilliance.Philips)	120	40	kernel D	1 mm	2 mm	skull—proximal tibial metaphysis	/	4.2	2.4
Wolf et al. 2014 ³	62	52	256-slice scanner (Brilliance iCT.Philips)	/	/	B40f	/	3 mm	skull—pelvis	/	9.4-11.3	2.4
Zacchino et al. 2015 ¹⁴	62	50	64—slice scanner (Somatom Definition. Siemens)	80	200-230	/	0.9 mm	1.5 mm	skull—tibial diaphysis	/	4.5	/
Zacchino et al. 2015 ¹⁴	67	50	16 slice CT (Brilliance.Philips) / 256 iCt Philips	120	40	/	2 mm	2 mm	skull—tibial diaphysis	/	4.2	/
Cretti et al. 2016 ¹⁵	67 ± 13	29	Philips Brilliance 64 slices	120/140	40	Standard	0.984	5 mm	skull to femura included	398	3.2	/
Borggreve et al. 2015 ¹⁶	/	128	64-slice CT scanner (Somatom Siemens)	120	100	/	/	1.5 mm	skull—knee	/	4-6.5	/
Gordic et al. 2014 ¹⁷	46.7 ± 20.7	120	64-slice CT scanner (Somatom Siemens)	120	250	FBP	1.6 mm	2 mm	single district	/	29.5	/
Mangiavalli et al. 2016 ¹⁸	/	318	16-slice CT scanner (no manufacturer)	120	40	/	1 mm	2 mm	skull—proximal tibial metaphysic	/	4.1	/
Lambert et al. 2017 ⁹	65.1 ± 10.7	74	256-slice scanner (Brilliance.Philips)	120	30	filter C kernel	0.993 mm	0.9 mm	skull—proximal tibial metaphysis	289 ± 85	2.7 ± 0.9	2.5 ± 0.9
Chrzan et al. 2017 ¹⁹	61	41	160-slice CT (Toshiba Aquilion PRIME)	120	86	FC35 kernel	0.813 mm	1 mm	skull—femoral bones	660-810	/	/
Suntharalingam et al. 2018 ²⁰	/	30	dual-source CT (Somatom Force. Siemens)	100	130	br64 kernel	/	1.5 mm	skull—proximal tibial metaphysis	96	1.45	/
Zambello et al. 2019 ²¹	57	18	128 Slice CT (Somatom Definition. Siemens)	120	35	B30f kernel	1 mm	2 mm	hands to feet	/	/	/
Simeone et al. 2019 ²²	68 ± 11	116	Multidetector CT (Siemens Force.GE Lightspeed)	120	40-70	bone kernel	1 mm	2.5 mm	skull to 2 cm below the knee joint	/	4.8 ± 1.5	2.04
Molinari et al. 2019 ²³	/	7	Philips Brilliance iCT 128 slices	120	/	/	/	/	2 scan from skull to feet	682	10	/
Hemke et al. 2020 ¹⁰	67.9	228	(Siemens.GE.Philips) assessed Somatom Force (Siemens)	120	70	/	1 mm	/	skull—pelvis	515	4.34	2.04
Franchi et al. 2020 ²⁴	/	30	256-slice CT scan no manufacturer	/	/	/	/	/	/	/	1.9	/

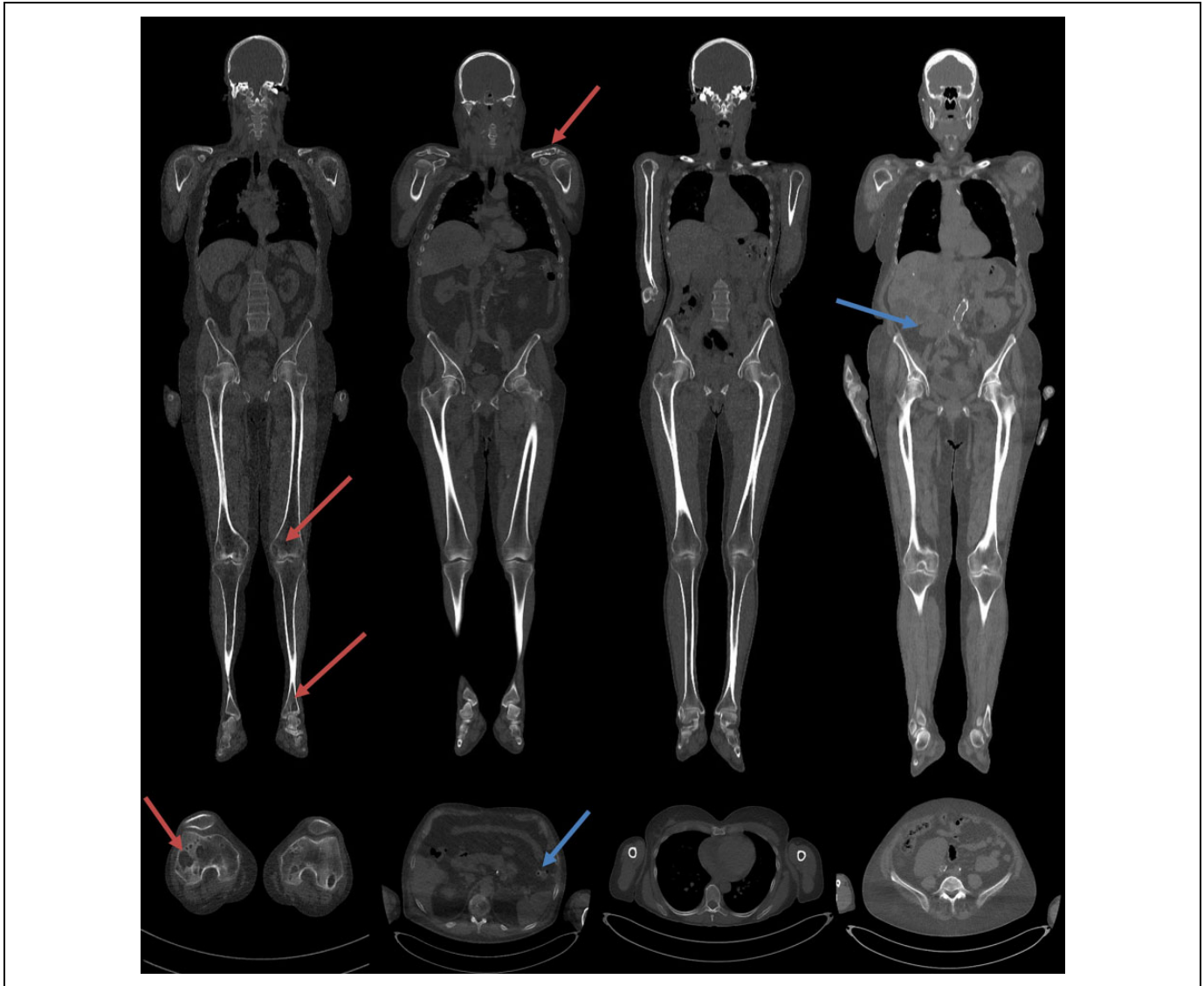


Figure 1. Coronal and sagittal reconstructions from WBLDCT scan. From left to right, on top of the coronal MPR images and bottom the axial images, a patient showed the presence of osteolytic lesions, a patient also with extra-osseous findings (diverticulum), the patient showed no osteolytic lesions and patients only with extra-osseous findings (ectopic kidney). Blue arrows show the osteolytic lesion, the reds show the extra-osseous findings.

choices,²⁶ which take advantages of early diagnosis and accurate staging.²⁷ Following the new IMWG criteria, it is of clinical importance to detect bone involvement in MM. Indeed, bone involvement is a significant cause of morbidity and mortality and a key indicator of prognosis in MM patients.⁸ Although skeletal radiographs have been used to assess MM patients' bone involvement, its limitations are well known and have been previously documented.²⁷

The extensive availability of multidetector CT scanners allowed the use of WBLDCT protocol for the diagnosis and follow-up of MM, where the reduced acquisition time (about 20 seconds) in possibly un-compliant patients is counterbalanced by ionizing radiation exposure. The coronal and sagittal MPR provide an excellent overview of the whole body,

allowing a better visualization of the spine and of vertebral compression fractures in the sagittal plane, and a clearer assessment of the medullary cavity and of focal or diffuse hyperdense myeloma deposits in the coronal one. Moreover, shifting to the soft tissue window visualization, in addition to the bone window, the analysis could be extended to the brain, lungs, and abdominal organs to highlight concomitant diseases (e.g., lung nodules, hepatosplenomegaly, accidental injuries) and extra-bone localizations.²⁸

In recent literature, WBLDCT protocols with estimated effective doses comparable with CSS have been described, employing kVp or mAs reductions, iterative reconstruction (IR) techniques, or spectral shaping. Horger et al. first described a WBCT study to assess therapy response in patients

with MM, demonstrating the more reliability of the CT approach compared to the conventional, laboratory-based follow-up.⁶ Then, further studies assessed the importance of a WBLDCT, in patient with MM, providing important information for the disease monitoring and management of patients,²² as long as detection of incidental findings.¹³

Multiple studies have been performed in order to optimize the protocol and provide a lower effective dose than the CSS.^{9,10,13,22,25-28} Several works tested different combinations of CT parameters in order to obtain a reliable and diagnostic protocol. Gleeson et al. tested combinations of kV that range from 80-140 kVp, and tube current-time product from 14-125 mAs with the modulation of the activated current and a moderately sharp reconstruction algorithm, to generate a low effective dose of about 1.74 mSv,²⁹ while Kropil et al. used a 100 kV and 100 mAs protocol, with automatic tube current modulation, to administer an effective dose of approximately 4.8 mSv.⁴ Most recent studies, instead, employ a 120 kV protocol and a tube current between 30 and 100 mAs, to achieve an effective dose ranging between 2.7 mSv⁹ and 29.5 mSv.^{4,6-10,12-18,21-23,25-32} Other studies have been focused on a different approach based on low tube voltage (80 kV) and high current (200–230 mAs), generating an effective dose of about 4.5 mSv.¹⁴

Saravanabavaan et al. exploited the potential of spectral shaping thanks to tin filter, in synergy with IR and automatic current modulation on a third-generation DSCT (Sn 100 kV, ref. mAs: 130). In their work, they compared the image quality and effective dose with patients who have been examined on a second-generation DSCT with a standard low-dose protocol (100 kV, ref. mAs: 111), demonstrating a good image quality and, more relevant, a reduction of radiation dose by approximately 74% compared to a similar protocol without tin filter.²⁰

After systematic literature reviewing relating to the WBLDCT and single-energy CT protocols with spectral filtration at 100 kV,^{15,17,18,20,23,33,34} we modified our protocol furtherly reducing the reference mAs, obtaining a mean effective dose of 0.44 mSv, lower than those reported in the literature for the same procedure, and mainly than CSS (ranges between 1.5 and 2.5 mSv.³⁰ Despite the reduction of the dose can generate a minor image quality due to the background noise increase, we reported a good/excellent image quality, also due to intrinsic bone contrast, also compared to osteolytic lesions, and reconstruction algorithms improvement.³⁵

Moreover, an added value of our protocol compared to the existing literature is that CT scans were acquired including feet, although WBLDCT acquisition recommendations, suggested to restrict the FOV size until the proximal metaphysis of the tibia.³⁰ Only 2 previous works^{22,27} extended the acquisition volume to the entire whole-body, reporting an effective dose of about 10 mSv, so at least 20 times that recorded in our study.

Our study shows that whole-body imaging without contrast agent injection at 100 kV with spectral modeling through a dedicated tin filter on the tube side allows the reduction in the radiation dose and consequently a lower effective dose. In the 2nd and 3rd generation DSCT, an additional tin filter allows

spectral modeling. On the second generation DSCT, this is traditionally used for better spectral separation when operating with dual-energy CT scans and not available for single energy CT.^{36,37} With the third generation DSCT this system can also be used in single energy-single source mode to optimize the X-ray spectrum in a system known as “spectral modeling.” This process removes low energy photons from the spectrum. Furthermore, the use of an improved third-generation IR algorithm reduces image noise and/or radiation dose while preserving image quality, compared to standard filtered back-projection reconstructions.^{38,39} Finally, the 3rd generation DSCT applies adaptive tube current modulation.⁴⁰

In our study, thanks to the combination of the use of a 3rd generation DSCT with tin filter, IR, and low reference mAs, we obtained a low radiation dose, without losing diagnostic sensitivity for the detection of osteolytic alterations.

In conclusion, the proposed WBLDCT protocol has the real potential to reduce radiation exposure, with a dose effective reduction ranging from 3 to 6 times compared with CSS. This feature becomes a non-negligible factor in management of patients with bone involvement, where strict follow-ups with CT scans can be needed.

Authors' Note

The opinions expressed in the presented article are our own and not an official position of the institution or funder.


Declaration of Conflicting Interests

The author(s) declared no potential conflicts of interest with respect to the research, authorship, and/or publication of this article.

Funding

The author(s) received no financial support for the research, authorship, and/or publication of this article.

ORCID iD

Dario Baldi  <https://orcid.org/0000-0001-7464-4499>

References

1. Silbermann R, Roodman GD. Myeloma bone disease: pathophysiology and management. *J Bone Oncol.* 2013;2(2):59-69.
2. Terpos E, Morgan G, Dimopoulos MA, et al. International Myeloma Working Group recommendations for the treatment of multiple myeloma-related bone disease. *J Clin Oncol.* 2013;31(18):2347.
3. Wolf MB, Murray F, Kilk K, et al. Sensitivity of whole-body CT and MRI versus projection radiography in the detection of osteolyses in patients with monoclonal plasma cell disease. *Eur J Radiol.* 2014;83(7):1222-1230.
4. Kröpil P, Fenk R, Fritz LB, et al. Comparison of whole-body 64-slice multidetector computed tomography and conventional radiography in staging of multiple myeloma. *Eur Radiol.* 2008;18(1):51-58.

5. Edlertson GA, Gillespie PJ, Grebbell FS. The radiological demonstration of osseous metastases. Experimental observations. *Clin Radiol*. 1967;18(2):158-162.
6. Horger M, Claussen CD, Bross-Bach U, et al. Whole-body low-dose multidetector row-CT in the diagnosis of multiple myeloma: an alternative to conventional radiography. *Eur J Radiol*. 2005;54(2):289-297.
7. Gleeson TG, Moriarty J, Shortt CP, et al. Accuracy of whole-body low-dose multidetector CT (WBLDCT) versus skeletal survey in the detection of myelomatous lesions, and correlation of disease distribution with whole-body MRI (WBMRI). *Skeletal Radiol*. 2009;38(3):225-236.
8. Rajkumar SV, Dimopoulos MA, Palumbo A, et al. International Myeloma Working Group updated criteria for the diagnosis of multiple myeloma. *Lancet Oncol*. 2014;15(12):e538-e548.
9. Lambert L, Ourednicek P, Meckova Z, Gavelli G, Straub J. Whole-body low-dose computed tomography in multiple myeloma staging: superior diagnostic performance in the detection of bone lesions, vertebral compression fractures, rib fractures, and extraskelatal findings compared to radiography with similar radiation exposure. *Oncol Letters*. 2017;13(4):2490-2494.
10. Hemke R, Yang K, Hussein J, Bredella MA. Organ dose and total effective dose of whole-body CT in multiple myeloma patients. *Skeletal Radiol*. 2020;49(4):549-554.
11. Chassang M, Grimaud A, Cucchi JM, et al. Can low-dose computed tomographic scan of the spine replace conventional radiography? An evaluation based on imaging myelomas, bone metastases, and fractures from osteoporosis. *Clin Imaging*. 2007;31(4):225-227.
12. Princewill K, Kyere S, Awan O, Mulligan M. Multiple myeloma lesion detection with whole body CT versus radiographic skeletal survey. *Cancer Invest*. 2013;31(3):206-211.
13. Ippolito D, Besostri V, Bonaffini PA, Rossini F, Di Lelio A. Diagnostic value of whole-body low-dose computed tomography (WBLDCT) in bone lesions detection in patients with multiple myeloma (MM). *Eur J Radiol*. 2013;82(12):2322-2327.
14. Zacchino M, Bonaffini PA, Corso A, et al. Inter-observer agreement for the evaluation of bone involvement on whole body low dose computed tomography (WBLDCT) in multiple myeloma (MM). *Eur Radiol*. 2015;25(11):3382-3389.
15. Cretti F, Perugini G. Patient dose evaluation for the whole-body low-dose multidetector CT (WBLDMDCT) skeleton study in multiple myeloma (MM). *Radiol Med*. 2016;121(2):93-105.
16. Borggreffe J, Giravent S, Campbell G, et al. Association of osteolytic lesions, bone mineral loss and trabecular sclerosis with prevalent vertebral fractures in patients with multiple myeloma. *Eur J Radiol*. 2015;84(11):2269-2274.
17. Gordic S, Morsbach F, Schmidt B, et al. Ultralow-dose chest computed tomography for pulmonary nodule detection: first performance evaluation of single energy scanning with spectral shaping. *Invest Radiol*. 2014;49(7):465-473.
18. Mangiacavalli S, Pezzatti S, Rossini F, et al. Implemented myeloma management with whole-body low-dose CT scan: a real life experience. *Leuk Lymphoma*. 2016;57(7):1539-1545.
19. Chrzan R, Jurczyszyn A, Urbanik A. Whole-Body Low-Dose Computed Tomography (WBLDCT) in assessment of patients with multiple myeloma-pilot study and standard imaging protocol suggestion. *Pol J Radiol*. 2017;82:356-363.
20. Suntharalingam S, Mikat C, Wetter A, et al. Whole-body ultra-low dose CT using spectral shaping for detection of osteolytic lesion in multiple myeloma. *Eur Radiol*. 2018;28(6):2273-2280.
21. Zambello R, Crimi F, Lico A, et al. Whole-body low-dose CT recognizes two distinct patterns of lytic lesions in multiple myeloma patients with different disease metabolism at PET/MRI. *Ann Hematol*. 2019;98(3):679-689.
22. Simeone FJ, Harvey JP, Yee AJ, et al. Value of low-dose whole-body CT in the management of patients with multiple myeloma and precursor states. *Skeletal Radiol*. 2019;48(5):773-779.
23. Molinari A, Pistoia F, Listo E, Ottolenghi S. Application of low-dose CT in myeloma multiple patients: dose reduction with optimized protocols. *Eur Congress Radiol*. 2019;C-0291.
24. Franchi M, Depaoli A, Guarnaccia C, et al. Image quality and dose evaluation in Whole-Body Low-Dose Computed Tomography (WBLDCT) in patients with multiple myeloma and related plasma cell dyscrasias. *EuroSafe Imaging*. 2020;ESI-03838.
25. Forte E, Monti S, Parente CA, et al. Image quality and dose reduction by dual source computed tomography coronary angiography: protocol comparison. *Dose-Response*. 2018;16(4):1559325818805838.
26. Kumar SK, Rajkumar SV, Dispenzieri A, et al. Improved survival in multiple myeloma and the impact of novel therapies. *Blood*. 2008;111(5):2516-2520.
27. Regelink JC, Minnema MC, Terpos E, et al. Comparison of modern and conventional imaging techniques in establishing multiple myeloma-related bone disease: a systematic review. *British J Haematol*. 2013;162(1):50-61.
28. Surov A, Bach AG, Tcherkes A, Schramm D. Non-osseous incidental findings in low-dose whole-body CT in patients with multiple myeloma. *British J Radiol*. 2014;87(1041):20140185.
29. Gleeson TG, Byrne B, Kenny P, et al. Image quality in low-dose multidetector computed tomography: a pilot study to assess feasibility and dose optimization in whole-body bone imaging. *Can Assoc Radiol J*. 2010;61(5):258-264.
30. Mouloupoulos LA, Koutoulidis V, Hillengass J, et al. Recommendations for acquisition, interpretation and reporting of whole body low dose CT in patients with multiple myeloma and other plasma cell disorders: a report of the IMWG Bone Working Group. *Blood Cancer J*. 2018;8(10):1-9.
31. Robert C, Jurczyszyn A, Urbanik A. Whole-body low-dose computed tomography (WBLDCT) in assessment of patients with multiple myeloma—pilot study and standard imaging protocol suggestion. *Polish J Radiol*. 2017;82:356.
32. Prins RD, Thornton RH, Schmidlein CR, Quinn B, Ching H. Estimating radiation effective doses from whole body computed tomography scans based on US soldier patient height and weight. *BMC Med Imag* 2011;11(1):20.

33. Haubenreisser H, Meyer M, Sudarski S, Allmendinger T, Schoenberg SO, Henzler T. Unenhanced third-generation dual-source chest CT using a tin filter for spectral shaping at 100 kVp. *Eur J Radiol.* 2015;84(8):1608-1613.
34. Suntharalingam S, Allmendinger T, Blex S, et al. Spectral beam shaping in unenhanced chest CT examinations: a phantom study on dose reduction and image quality. *Academic Radiol.* 2018; 25(2):153-158.
35. Chantry A, Kazmi M, Barrington S, et al. Guidelines for the use of imaging in the management of patients with myeloma. *British J Haematol.* 2017;178(3):380-393.
36. Primak AN, Ramirez Giraldo JC, Liu X, Yu L, McCollough CH. Improved dual-energy material discrimination for dual-source CT by means of additional spectral filtration. *Med Physics.* 2009; 36(4):1359-1369.
37. Ravi KK, Platt JF, Cohan RH, Caoili EM, Al-Hawary MM, Wasnik A. Dual-energy CT with single-and dual-source scanners: current applications in evaluating the genitourinary tract. *Radiographics.* 2012;32(2):353-369.
38. Antonio M, Takx RA, Schoepf UJ, et al. Coronary CT angiography: image quality, diagnostic accuracy, and potential for radiation dose reduction using a novel iterative image reconstruction technique—comparison with traditional filtered back projection. *Eur Radiol.* 2011;21(10):2130.
39. Hara Amy K, Paden RG, Silva AC, Kujak JL, Lawder HJ. Iterative reconstruction technique for reducing body radiation dose at CT: feasibility study. *Am J Roentgenol.* 2009;193(3):764-771.
40. Kalra MK, Maher MM, Toth TL, et al. Techniques and applications of automatic tube current modulation for CT. *Radiol.* 2004; 233(3):649-657.